# Laboratori Nazionali di Frascati

LNF-88/25(R)
30 Maggio 1988

M. Pelliccioni:

## RADIATION PROTECTION PROBLEMS IN THE DESIGN OF THE LISA PROJECT

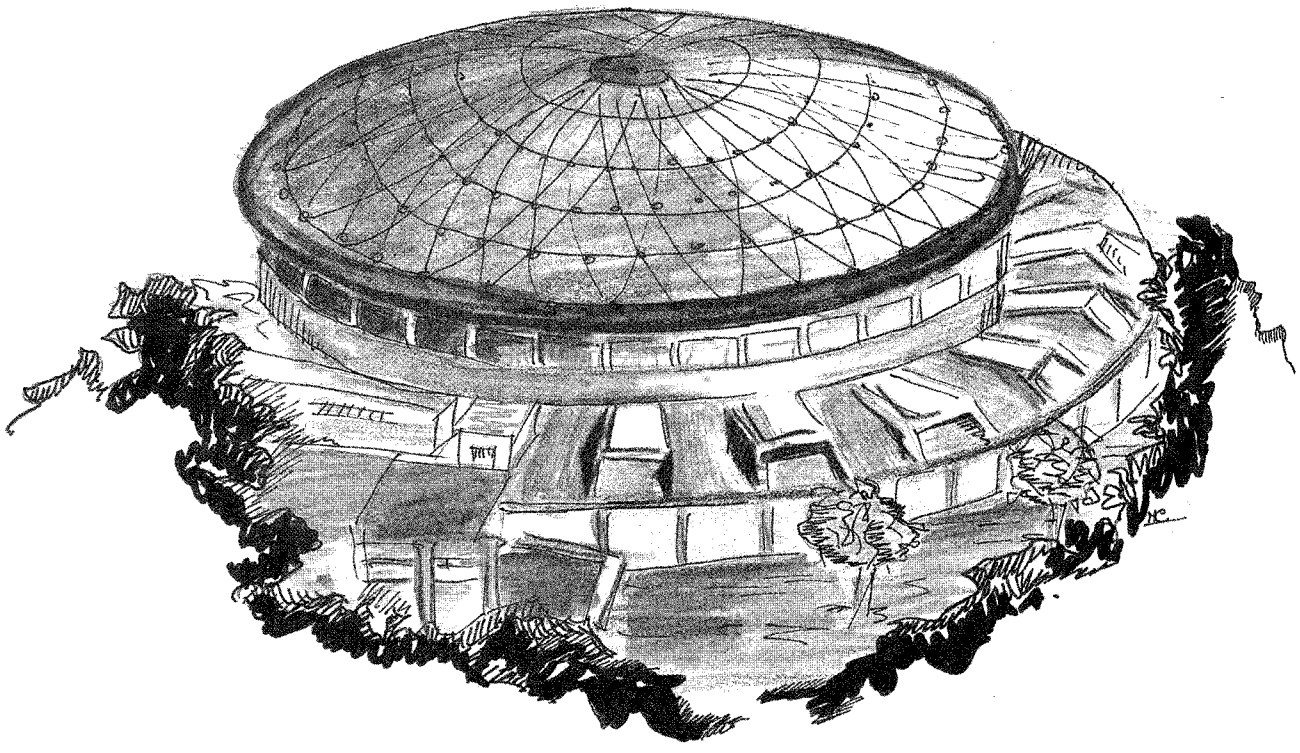

**Servizio Documentazione**
**dei Laboratori Nazionali di Frascati**
**P.O. Box, 13 - 00044 Frascati (Italy)**

INFN - Laboratori Nazionali di Frascati
Servizio Documentazione

LNF-88/25(R)
30 Maggio 1988

# RADIATION PROTECTION PROBLEMS IN THE DESIGN OF THE LISA PROJECT

M. Pelliccioni
INFN - Laboratori Nazionali di Frascati, P.O.Box 13, 00044 Frascati (Italy)

## 1. - INTRODUCTION

The superconducting linear accelerator known as LISA (Linear Superconducting Accelerator, Version A) is to be located at the INFN Frascati Laboratories (LNF) (see Fig.1).

The LNF area surrounding the machine is bounded on the north-east by a secondary road lying about 20 m from the machine itself. Beyond the road and to the south-east, the land is given over to agriculture. The nearest LNF building structures are the workshops situated north-west and south-west about 40 m from the machine. A new workshop will be located at a distance of about 10 m.

## 2. - DESCRIPTION OF THE PLANT

The whole plant comprises:

- an accelerator room, referred to in the following as the LISA Hall, located underground and walled in with ordinary concrete and soil;
- a generator room;
- a technical workshop.

Fig. 2 illustrates the layout of the premises and building structures.

The accelerator to be located in the LISA Hall consists of:

- an electron source;
- a 1 MeV pre-accelerator;
- four superconducting accelerator cavities capable of transmitting an energy of 25 MeV (at 5 MV/m) or 36 MeV (at 7.5 MV/m) to the particles;
- a beam recirculation ring to double the energy.

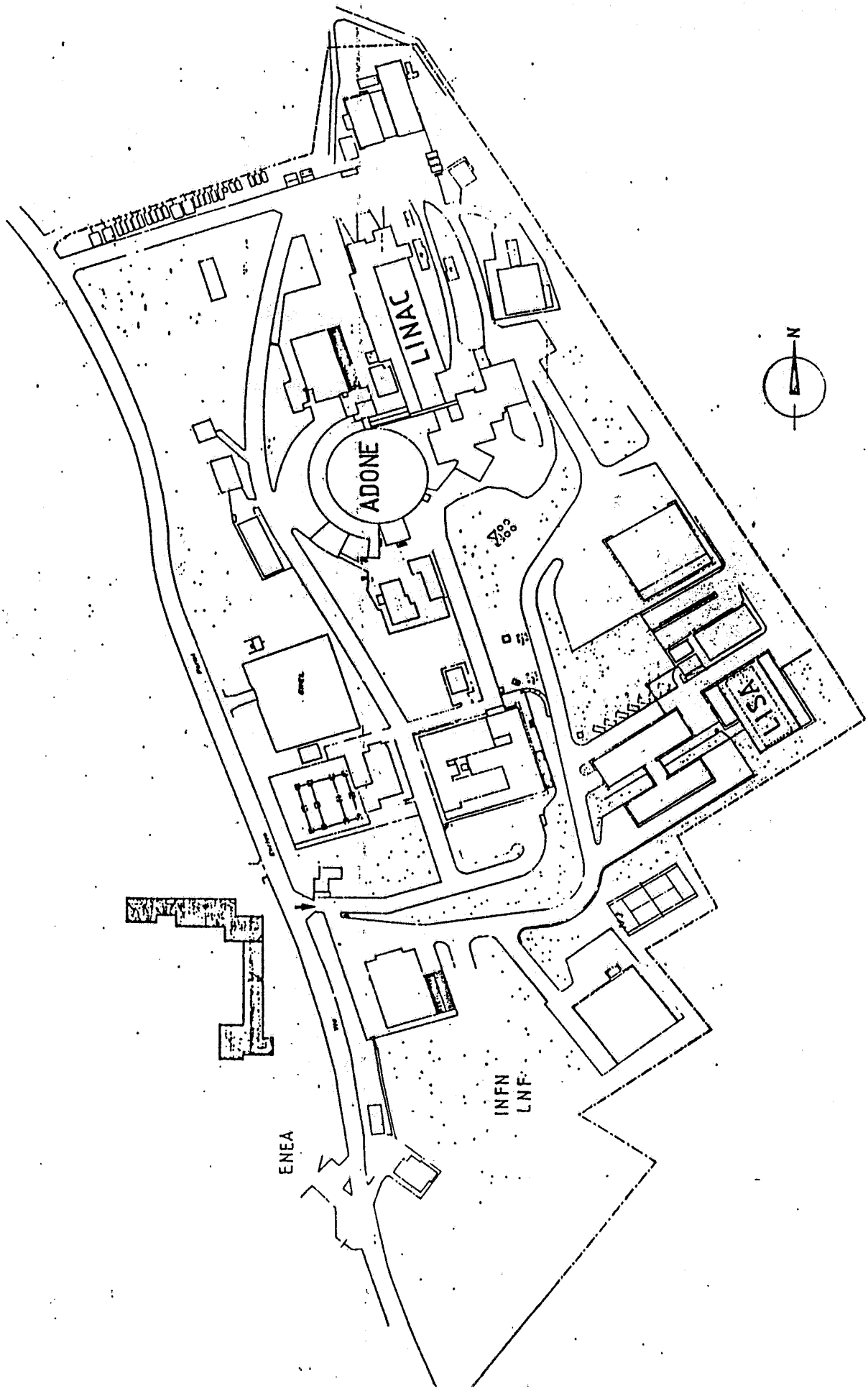


FIG. 1 - Planimetry of the LNF.

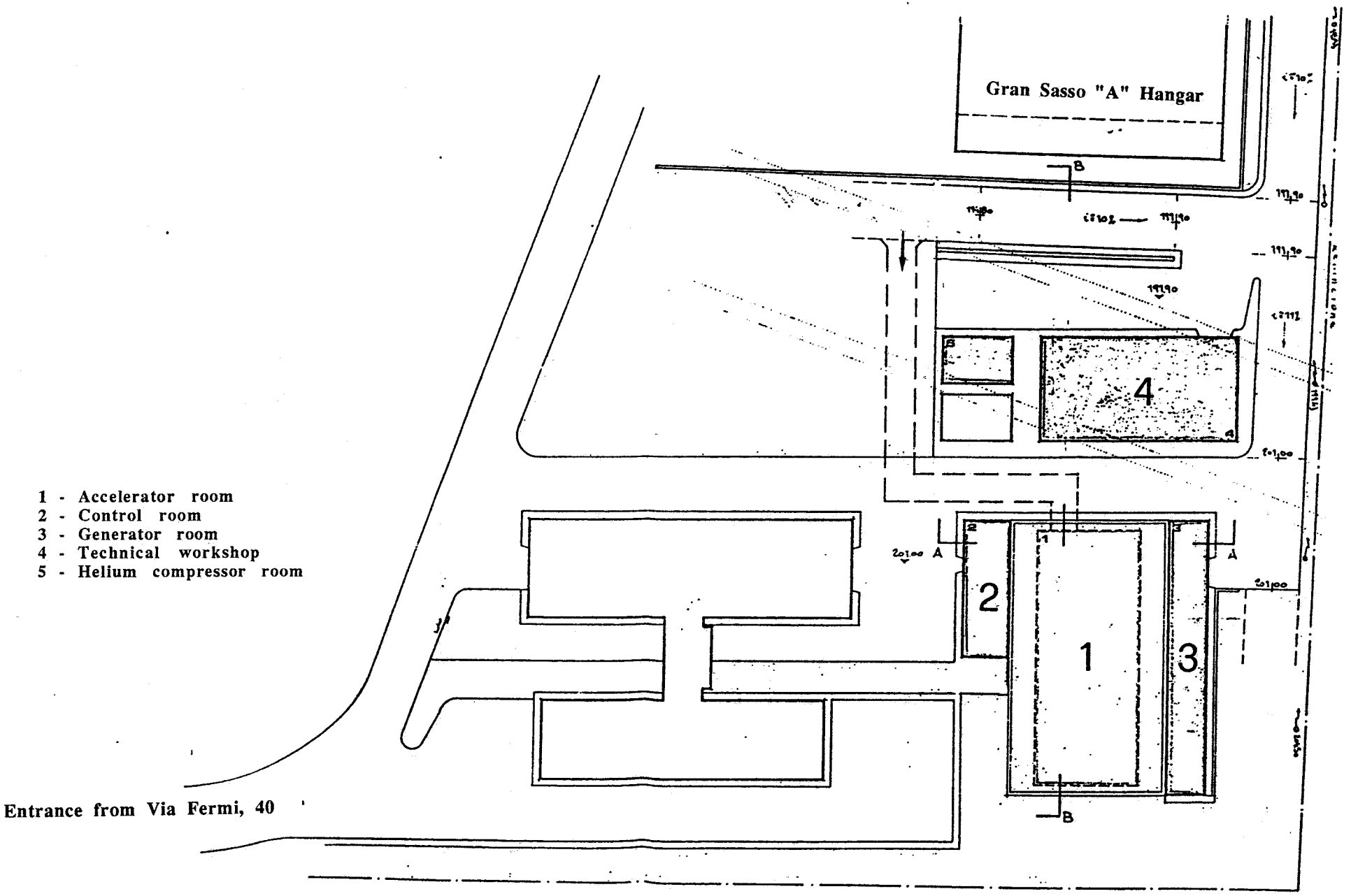


FIG. 2 - Layout of the premises and building structures.

All the above elements are connected by a vacuum guide for the travelling electrons. A ondulator magnet will be located along the exit path for the production of a laser beam. The beam path will terminate in appropriate beam stops.

The vacuum guide tubes are 2-mm-thick steel. The pre-injector is 1-cm-thick copper. The 2.5-mm-thick niobium cavities are immersed in a liquid helium bath at 4.6 $^{o}$K and are contained in a steel and aluminium cryostat of total thickness 10 cm.

The cooling tubes transporting water and helium, the RF waveguides and the various electric cables will lead into the LISA Hall.

The control room, generator room and technical workshops are located to the sides of the Hall and raised above it by about 4 m (ground level).

The LISA Hall has two means of access. The main entrance consists of a 3-leg corridor or labyrinth leading from the secondary road. The corridor ends in a sliding door which is subject to the system of safety controls. The same system controls the entrance from the road.

The second access to the Hall is via three flights of stairs which connect the Hall to a corridor terminating in an exit stairway. As for the above entrance, two safety-controlled doors will be put in, one leading from the road and one from the LISA Hall.

The control room is at ground level and houses the computer and accelerator control terminals.

The generator room houses the magnet power supply, the klystrons, the helium refrigerator, the ventilation fans and the closed circuit water pumps. As this room contains radioactive apparatus, access will be subject to the proper regulations. The helium compressors will be installed in an appropriate building outside the room.

The various machine parts will be assembled in the technical workshop.

## 3. - DESCRIPTION OF THE MACHINE AND OTHER RADIATION SOURCES

The operational characteristics of the linac are as follows:

- Maximum energy 73 MeV
- Average current 10-130 μA

The current will be a sequence of pulses of variable length and repetition within the limits of the above average value.

In the setup phase, the beam, with an energy between 36 MeV and 73 MeV, can be entirely lost in any part of the ring. At steady state, the losses should be contained within 10%. It is, however, essential to reduce the losses as much as possible because the superconducting cavities cannot operate correctly when the dissipative power exceeds values of the order of one watt.

The characteristics of the radiation sources produced in the points where the above-mentioned losses occur are described in sections 4 and 5.

The superconducting cavities will have a maximum electric field of 7.5 MV/m and will themselves be X-ray sources. Radiation emission from this type of apparatus is undesirable and erratic and not easy to quantify.

Dose rates measured around this kind of cavity of over 10 $Gyh^{-1}$ at one meter are quoted in the literature (CEBAF 86). In fact, in RF cavities, electrons are produced mainly due to field effects and, after acceleration along the electric lines of force, collide with the walls where they are absorbed and give rise to X rays.

The radiation intensity outside the cryostat depends on several physical parameters such as the supply voltage, the injected power, the vacuum conditions, the thickness and characteristics of the walls, and other difficult-to-quantify but not less important factors like the condition of the walls. In fact, the number of electrons emitted depends on the treatment and cleaning of the walls. Thus, keeping the cavity supplied, the number of electrons decreases with time due to the effect of the conditioning of the cavity itself.

It has been observed that the intensity of the radiation emitted increases according to a power-law with the applied electric field, and linearly with injected power.

However, the radiation produced in the superconducting cavities does not affect the design for the shielding whose dimensions have to be based on the major sources originating from the accelerator beam. It is important, however, that the cavities are not supplied when personnel have access to the accelerator room.

The klystrons in the generator room are further sources of radiation:

- n.1 with a voltage of 50 kV and a current of 10 A;
- n.2 with a voltage of 20 kV and a current of 10 A.

Each klystron will be shielded with lead like the ones at the linac currently operating.

## 4. - SHIELDING

### 4.1. - Estimates of shielding thicknesses

As the room where the machine is to be installed is underground, the evaluation of the efficiency of the shields to be adopted will be carried out essentially with regard to the external area overhead. The maximum design parameters are considered for the energy and current of the accelerated electron beam ( E=73 MeV, i=130 μA, P=9.49 kW).

In order to calculate the shielding, the following components of the radiation field must be considered:

a) bremsstrahlung X-ray emission;
b) photoneutrons from excitation of the giant resonance.

Under the worst of hypothesis it is supposed that the whole beam can be lost with continuity at a point in one of the bends of the machine. This is obviously an extreme hypothesis and even if such a situation should occur, it could only last for a short time as it is completely anomalous and inacceptable for experimental purposes. It is also definitely conservative with respect to the more probable case of loss along part or all of the machine. For further prudence, it is also supposed that

the X-ray and neutron emission is the maximum possible, as would occur for a beam hitting a high-Z thick target , optimized for the maximum production of secondary radiation.

In the case of 33 MeV, 100 MeV and 5 GeV electron beams hitting this type of target, the experimental data relative to the absorbed dose rate $\dot{D}$ expressed in $Gyh^{-1}$ have been arranged to obtain the following empirical rule for the various parameters involved (CERN 84):

$$\dot{D} = 2.7\ PR^{-2}E^{1/2}\theta^{-3/2} \qquad (1)$$

where E is the energy of the incident electrons, P the beam power in watts, R the distance in meters of the point of interest from the target in the direction forming an angle $\theta$ with the beam direction.

Equation (1) can be held valid for angles which differ sufficiently from $0^o$, between about $10^o$-$20^o$ and $90^o$.

In this calculation the right-hand side of Eq. (1) should be further multiplied by a factor 2 to take into account the suggestions in the IAEA Report 188 (IAEA 79).

With regard to giant resonance neutrons, whose angle distribution is practically isotopic, the data available in the literature (IAEA 79, CEBAF 86, etc.) lead one to assume a source term equal to 11.5 $Sv\ h^{-1}m^2kW^{-1}$. In view of the current debate on the eventual increase of the neutron quality factor and of the proposals put forward in this regard (ICRP 85, ICRU 86, ICRP 87), it has been thought opportune to multiply this term by a factor 2:

$$\dot{H}_o = 23\ Sv\ h^{-1}\ m^2\ kW^{-1} \qquad (2)$$

Ordinary concrete is used as shielding material in the present calculation ($\rho$ = 2.35 $gcm^{-3}$). In practice, however, it is customary to use this material for only a part of the general shielding as it is more economic to substitute it partly with soil. The necessary soil thickness can be obtained from the thickness of the ordinary concrete using a ratio scale of the respective densities. Lead will be used for the shielding of particular areas (e.g., beam stops).

The parameter values needed to describe the attenuation of the two components of the radiation field in the two materials are given in Table I.

**TABLE I** - Tenth-values layers (TVL) and attenuation lengths ($\lambda$) used in the calculation (data taken from Sw 85).

| *Type of radiation* | *Material* | *Density ($gcm^{-3}$)* | *TVL(cm)* | *$\lambda$(cm)* |
|---|---|---|---|---|
| X rays | Ordinary concrete | 2.35 | 47 | 20.4 |
| | Lead | 11.35 | 5 | 2.2 |
| Giant resonance neutrons | Ordinary concrete | 2.35 | 39 | 16.9 |

With reference to Fig. 3, where t is the thickness of the shield above the machine and h is the distance between the beam level and the inside surface of the shielding (4.2 m), the contributions to the dose equivalent (expressed in μSv $h^{-1}$), due to X rays and neutrons in a point P on the outside surface of the shield in the direction θ , with the hypotheses adopted, are respectively:

$$\dot{H}_\gamma = 5.4 \cdot 10^9 \, P \frac{\sin^2 \theta}{(t+h)^2} \exp\left(-\frac{t}{\lambda \sin\theta}\right) E^{1/2} \, \theta^{-3/2} \qquad (3)$$

$$\dot{H}_n = 2.3 \cdot 10^7 \, P \frac{\sin^2\theta}{(t+h)^2} \exp\left(-\frac{t}{\lambda \sin\theta}\right) \qquad (4)$$

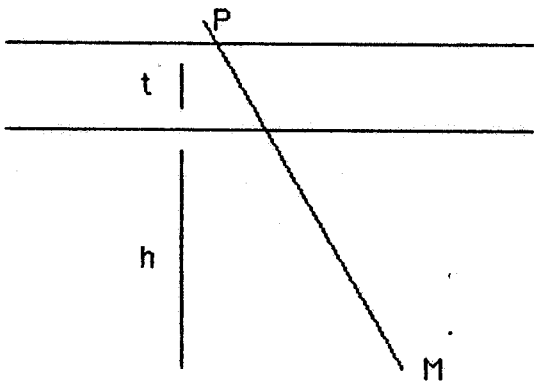


FIG. 3

These contributions are maximum in the direction at 90° where the effective shield thickness is minimum.

Fig. 4 shows the behavior in this direction of the dose equivalent for each of the two components ($\dot{H}_\gamma$ and $\dot{H}_n$) and their sum ($\dot{H}_{tot} = \dot{H}_\gamma + \dot{H}_n$), as a function of the thickness t of the shield.

The design objective is that $\dot{H}_{tot}$ not exceed 1 μSv $h^{-1}$, so the shield thickness must not be less than about 3.5 m of ordinary concrete. A value of $\dot{H}_{tot}$ = 0.22 μSv $h^{-1}$ corresponds to this thickness.

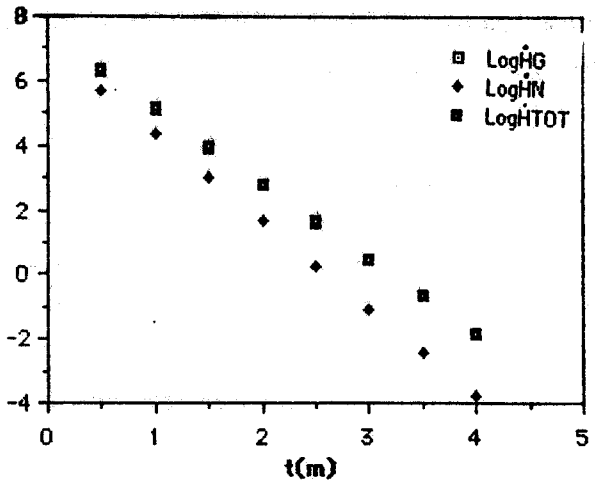


FIG. 4 - Gamma, neutron and total dose equivalent rate as a function of the thickness of the shield.

The thickness of the shield to be installed above the machine (75 cm of ordinary concrete and 415 of soil) equals about 393 cm of concrete, to which a dose equivalent even inferior to the one indicated above corresponds.

The doses in the other directions are less than the one at 90°, as shown in Fig. 5.

As the shielding everywhere is equal to at least 3.5 m of ordinary concrete, the dose equivalent expected in other areas (control room, generator room) will be even more modest than on the roof.

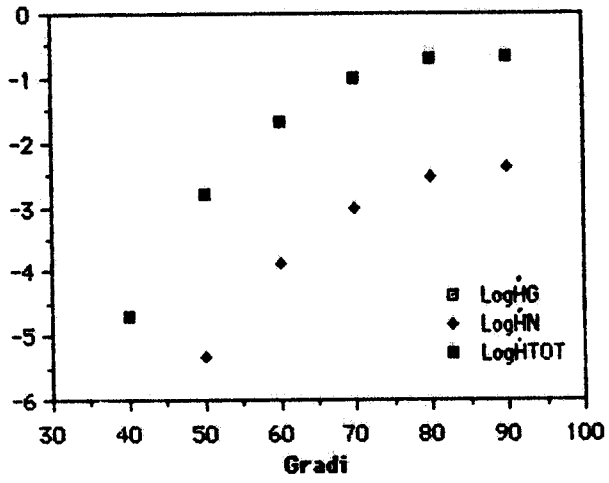


**FIG. 5** - Gamma, neutron and total dose equivalent rate as a function of the direction.

It should be noted that in the rather conservative hypothesis of 3000 hours' machine operation per year with the conditions for the preceding calculation, there would be a dose equivalent of less than 660 μSv/year in the area above the machine, so it is not worthwhile carrying out calculations relative to the skyshine effect.

### 4.2. - Beam stops

As already mentioned, the beam path will terminate in suitable beam stops and pass inside metal guides to reduce the air activation. The beam stops will consist of a 15-20-cm-thick lead nucleus able to attenuate the electromagnetic component by a factor of $10^3$ -$10^4$ surrounded by a layer of 50-cm-thick ordinary concrete to reduce any eventual exposure of personnel to radioactivity induced in the lead (see the following section 5.1). It should be recalled that the dose equivalent produced by an electron beam of 73 MeV bombarding a thick target in a direction at 0° is about $10^3$ times greater than at 90°, for an equal distance from the target.

### 4.3. - Labyrinths

As already reported in section 2, the main entrance to the LISA Hall consists of a 3-leg labyrinth with sections $A_1 = A_2 = 7.5$ m$^2$ and $A_3 = 9$ m$^2$, and length equal to about $r_1 = 5.5$ m, $r_2 = 25.5$ m and $r_3 = 38$ m.

The calculations of the doses transmitted along the labyrinth are made assuming, in the worst of cases as usual, that all the beam power is casually lost on a heavy target situated in the part of the machine nearest to the beam (about 6 m) and in the neighbourhood of its entrance. The source terms are therefore the same as those already discussed in Sect. 4.1.

For the study of neutron transmission, the universal curves based on a large amount of experimental data and proposed in this regard at CERN (St 87) have been used. The data are given in Fig. 6 for the first leg and in Fig. 7 for the successive ones.

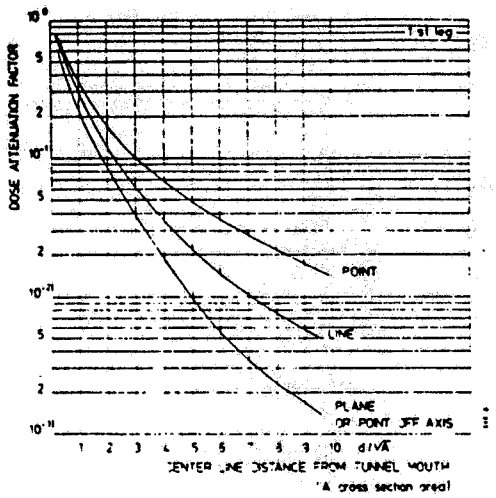


**FIG. 6** - Universal trasmission curves for the first leg of a labyrinth (da St 87).

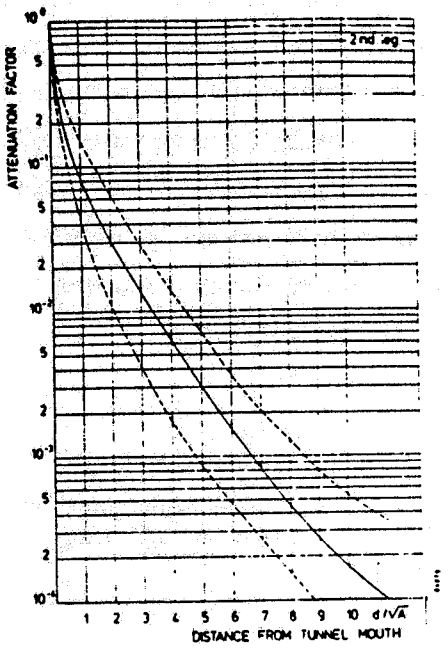


**FIG. 7** - Universal trasmission curves for the second and subsequent leg of a labyrinths (da St 87).

At the labyrinth exit, the dose equivalent $\dot{H}_{un}$ is therefore

$$\dot{H}_{un} = \frac{\dot{H}_o}{a^2} f_1(r_1)\, f_2(r_2)\, f_3(r_3) \qquad (5)$$

where a is the distance source-entrance of the labyrinth, and $f_1(r_1)$, $f_2(r_2)$, $f(r_3)$ are the attenuation factors relative to each of the 3 legs forming the labyrinth, assumed equal to $2.10^{-1}$, $2.10^{-4}$ and $2.10^{-5}$ respectively, from the curves in Figs. 6 and 7.

One therefore gets $\dot{H}_{un} \cong 1.4 \cdot 10^{-2} \mu Sv\ h^{-1}$, which is acceptable in view of the hypotheses adopted for the source terms.

Still more modest values are obtained using the following expression, based on experimental measurements made at the DESY accelerator (Te 82):

$$\dot{H}_{un} = \dot{H}_a \frac{2a^2}{(r_1 + a)^2} f_2(r_2)\, f_3(r_3) \qquad (6)$$

where:

$$f_2(r_2) = 2\left(e^{-r_2/0.45} + 0.022\, A_2^{1.3}\, e^{-r_2/2.35}\right) / \left(1 + 0.022\, A_2^{1.3}\right) \qquad (7)$$

$$f_3(r_3) = \left(e^{-r_3/0.45} + 0.022\, A_3^{1.3}\, e^{-r_3/2.35}\right) / \left(1 + 0.022\, A_3^{1.3}\right) \qquad (8)$$

and $\dot{H}(a)$ is the dose equivalent at the labyrinth entrance.

With regard to the gamma radiation, the inverse-square law has been used to calculate the attenuation in the first leg, while for the other two legs, the results of the calculations made at CERN using the Morse code (Fa 87) have been adopted. According to these calculations, a universal curve can also be proposed for the photon attenuation (Fig. 8).

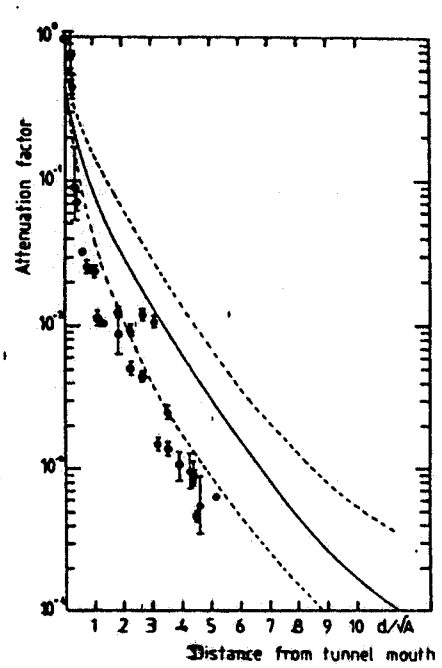


**FIG. 8** - Universal trasmission curves and calculated dose equivalent attenuation through successive legs of a LEP access way (da Fa 87).

One can therefore write:

$$\dot{H}_{n\gamma} = \dot{H}(a) \frac{a^2}{(r_1 + a)^2} f'_2(r_2) f'_3(r_3) \qquad (9)$$

where the symbols have an obvious meaning and obtain $\dot{H}_{u\gamma} \cong 0.1 \mu Sv\ h^{-1}$.

An analogous procedure can be followed to calculate the dose along the other access route which consists of three flights of stairs 2 m, 4.7 m and 3 m long respectively. However, the contributions from the two components of the radiation field considered are negligible, as in this case as well, the source is not situated in front of the labyrinth entrance.

### 4.4. - Ducts

Experience at numerous other accelerators has shown that no particular precautions are necessary regarding the ducts in the shielding (RF waveguides; electric cables; tubing for the systems and plants) as long as the ducts are not at the same level as the accelerator beam (see, e.g., CEBAF 86 or Te 87). It may be advisable to construct the ducts with an elbow of at least $90^o$ when they are situated near points where there is notable beam loss.

However, the addition of local shielding where higher than desired radiation levels occur is adequate enough for the ducts in question.

These straightforward regulations will be followed in realizing the ducts for the LISA plant.

# 5. - INDUCED RADIOACTIVITY

## 5.1. - Machine components

In order to calculate the induced radioactivity in the machine components accurately, it would be necessary to know numerous parameters with a precision difficult to obtain a priori. In fact, apart from the current and electron beam energy, one would have to know the material characteristics and geometry, the impurities present, operational conditions (time of operation, shutdowns), loss distribution, etc.

However, useful estimations for radiation protection purposes can be obtained using some simplifying hypothesis. In the first place, one can suppose the accelerator operation schematized in a series of regular cycles, as shown in Fig. 9, where the machine operates for a time T (equal to about 8 hours) and stops for a time t (about 16 hours). It is also supposed that the materials are impurity-free. Although this hypothesis rarely occurs in practice, it is sufficient for the present scope.

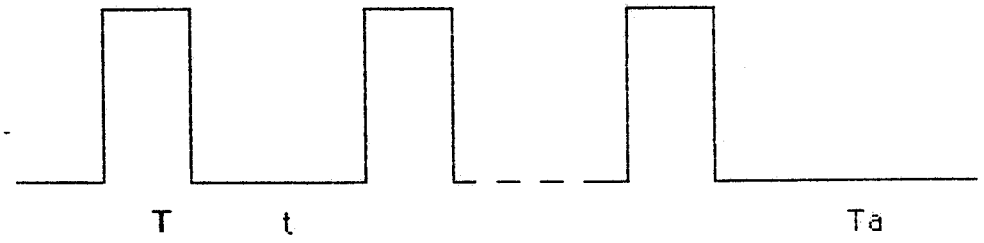


**FIG. 9** - Scheme of the accelerator operation.

Table II reports the saturation activity ($A_S$) for some of the materials most frequently used in accelerator construction, calculated with the hypothesis of continuous operation with a 1kW electron beam bombarding targets thick enough to allow the complete development of the electromagnetic cascade (IAEA 79). Only the most significant radionuclides have been listed for each material, neglecting in particular the ones with a short mean life which decay before entering the accelerator room. The same table shows the dose equivalent for each radionuclide at one meter from the target ($\dot{H}_S$), having neglected the self-absorption of the target itself.

Under the hypothesis of a sufficiently large number of operational cycles of the type described, the activity A for a radionuclide with a decay constant $\lambda$, after a waiting time $T_a$ taken from the end of irradiation, is given by :

$$A = \frac{A_s (1 - e^{-\lambda T}) e^{-\lambda T_a}}{1 - e^{-\lambda (T+t)}} \qquad (10)$$

The contribution to the dose equivalent $\dot{H}$ for the same radionuclide one meter from the target is in turn expressed by:

$$\dot{H} = \frac{A}{A_s} \dot{H}_s \qquad (11)$$

**TABLE II** - Saturation activity and dose equivalent one meter from thick targets of different materials (data taken from IAEA 79).

| *Material* | *Radionuclide* | $T_{1/2}$ | $A_s$ *(GBq kW$^{-1}$)* | $\dot{H}s$ *(mSv h$^{-1}$ m$^2$ kW$^{-1}$)* |
|---|---|---|---|---|
| *Aluminium* | Be-7 | 53.6g | 4.8 | 0.04 |
| | Na-22 | 2.62a | 9.3 | 3 |
| | Na-24 | 14.96h | 10 | 5.1 |
| *Iron* | Sc-46 | 83.9g | 7.4 | 2 |
| | V-48 | 16g | 15 | 8 |
| | Cr-51 | 27.7g | 15 | 3 |
| | Mn-52 | 5.6g | 1.3 | 0.39 |
| | Mn-54 | 303g | 22 | 7 |
| | Mn-56 | 2.58h | 1.2 | 0.27 |
| | Fe-52 | 8.2h | 2.1 | 0.4 |
| | Fe-56 | 2.6a | 490 | 90 |
| *Nickel* | Ni-56 | 6.1g | 3.7 | 1.6 |
| | Co-56 | 77.3g | 3.7 | 2.2 |
| | Ni-57 | 36h | 218 | 79 |
| | Co-57 | 270g | 218 | 75 |
| | Co-60 | 5.26a | 3.7 | 1 |
| *Copper* | Co-58 | 71.3g | 24 | 3.7 |
| | Co-58m | 9.2h | 24 | 2.1 |
| | Co-60 | 5.26a | 24 | 8.3 |
| | Ni-63 | 92a | 17 | 0 |
| | Cu-61 | 3.32h | 32 | 6.1 |
| | Cu-64 | 12.8h | 185 | 19 |
| *Lead* | Tl-204 | 3.81a | 0.9 | 0 |
| | Pb-202 | 3.62h | 2.2 | 0.3 |
| | Pb-203 | 52.1g | 31 | 1.3 |
| | Pb-204m | 1.1h | 89 | 14 |
| *Concrete* | Na-22 | 2.62a | 3.7 | 1.2 |

Equations (10) and (11) have been used to estimate the dose equivalent due to activity induced in the materials listed in Table II. The results of the calculations are shown in Table III for different values of the "cooling" time $T_a$. Obviously, for $T_a$=0, it would also be reasonable to consider radionuclides with a short or very short mean life, but they have been ignored here for the reasons already given.

Using the data in Table III, an indicative evaluation can be attempted for the dose levels which may be found around the most representative structures of the machine. For this purpose, one assumes an average operational power of 1 kW and power losses of the order of 10% on the structures considered.

**TABLE III** – Dose equivalent rate (mSv $h^{-1}kW^{-1}m^2$) due to induced radioactivity, one meter from thick targets of different materials where 10% of the beam is lost, for different values of the "cooling" time.

| $T_a(h)$ | *Aluminium* | *Concrete* | *Copper* | *Iron* | *Nickel* | *Lead* |
|---|---|---|---|---|---|---|
| 0 | 2.39 | 0.4 | 19.31 | 38.19 | 57.11 | 14.56 |
| 1 | 2.33 | 0.4 | 17.8 | 37.95 | 56.51 | 8.03 |
| 24 | 1.45 | 0.4 | 6.7 | 35.02 | 45.7 | 0.43 |
| 168 | 1 | 0.4 | 3.92 | 32.86 | 27.04 | 0.4 |
| 720 | 1 | 0.39 | 3.66 | 32.06 | 24.08 | 0.29 |
| 8760 | 0.98 | 0.3 | 2.45 | 24.02 | 10.12 | 0 |

*5.1.1. - Vacuum guide*

The vacuum guide is made of 2-mm-thick steel, equal to about 0.1 radiation length. The induced radioactivity in the steel can be estimated starting with its components. The radioactivity is largely due to nickel which is of the order of 12%, and to iron, of the order of about 66%. For simplicity's sake, the other components - the most important of which is chromium for about 17% - are neglected

In calculating the activity and, therefore, the doses, account must be taken of the fact that in this case the target is much thinner than what would be necessary to assure complete absorption of the electromagnetic cascade. The radioactivity reported in Table III for the different radionuclides produced in the nickel and iron must therefore be multiplied by a suitable reduction factor which as inferred from Fig. 10 is equal to about 0.018.

If the hypothesis is made that the 10% beam loss is concentrated in one point, the doses shown in Table IV are obtained.

Lower levels would obviously be obtained hypothesizing the loss distributed all along the machine.

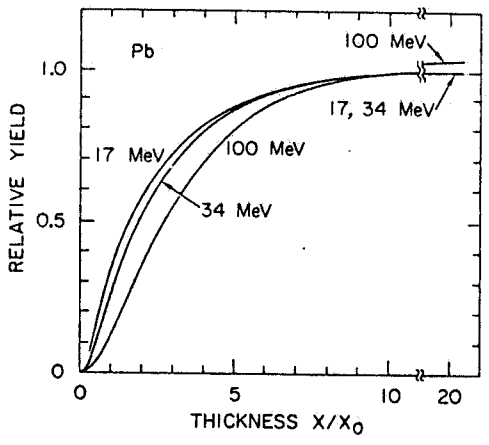


**FIG. 10** - Activity induced by electrons on thin targets (da IAEA 79).

**TABLE IV** - Dose equivalent rate, from induced radioactivity, 1 meter from a point on the vacuum guide where 10% of the beam is lost, for different values of of the "cooling" time.

| $T_d(h)$ | $\dot{H}$ $(mSv \cdot h^{-1} \cdot m^2)$ |
|---|---|
| 0 | 0.059 |
| 1 | 0.058 |
| 24 | 0.052 |
| 168 | 0.045 |
| 720 | 0.044 |
| 8760 | 0.031 |

*5.1.2. - Magnets*

The magnets are made from iron and resins and the coils are of copper.

The iron thickness is considered sufficient to assure complete absorption of the electromagnetic cascade. A reduction factor equal to 0.5 is used for the copper and evaluated adopting the same procedures described for the vacuum guide. The presence of resins is neglected.

In the case where it is hypothesized that the 10% beam loss occurs in correspondence to one of the magnets, the dose levels occurring 1 meter of distance away are those indicated in the 2nd column of Table V, having neglected the self-absorption in the magnet itself which is fairly significant in this situation.

**TABLE V** - Dose equivalent rate due to induced radioactivity one meter from the magnets under the hypothesis of a 10% beam loss, for different values of the "cooling" time.

| $T_d(h)$ | $\dot{H}$ $(mSv \cdot h^{-1} \cdot m^2)$ | $\dot{H}$ $(mSv \cdot h^{-1} \cdot m^2)$ |
|---|---|---|
| 0 | 4.8 | 0.13 |
| 1 | 4.7 | 0.13 |
| 24 | 3.8 | 0.10 |
| 168 | 3.5 | 0.097 |
| 728 | 3.4 | 0.094 |
| 8760 | 2.5 | 0.069 |

As there are 36 magnets, putting the most reasonable hypothesis that the losses are uniformly distributed, one would have the doses given in the third column of Table V.

Due to the conservative hypothesis introduced in the calculation, the expected doses should, nevertheless, be a good bit lower.

Whenever a notable loss is registered in correspondence to a particular magnet, it will be shielded to sufficiently reduce the dose levels around it.

*5.1.3. - Lead inside the beam stops*

In this case, it is useful to consider all the beam power and that the target is thick. Neglecting as usual self-absorption, one obtains the results given in Table VI.

**TABLE VI** - Dose equivalent rate due to induced radioactivity one meter from the beam stops, for different values of the "cooling" time.

| $T_a$ (h) | $\dot{H}$ (mSv·h$^{-1}$·m$^2$) | $\dot{H}_{conc.}$(mSv·h$^{-1}$·m$^2$) |
|---|---|---|
| 0 | 14.56 | 0.071 |
| 1 | 8.03 | 0.038 |
| 24 | 0.43 | 0.001 |
| 168 | 0.40 | —— |
| 720 | 0.29 | —— |
| 8760 | —— | —— |

The nucleus inside the beam stops is of lead and will be surrounded by at least 50 cm of ordinary concrete. Taking into account the attenuation in the concrete, the dose levels will lower towards values indicated in the third column of Table VI.

*5.1.4. - Concrete walls*

Putting the hypothesis that 10% of the beam is systematically lost in one of the walls of the accelerator room, the doses given in Table VII would be obtained.

**TABLE VII**- Dose equivalent rate, produced by induced radioactivity, one meter from the concrete walls at a point where a 10% beam loss occurs, for different values of "cooling" time.

| $T_a$ (h) | $\dot{H}$ (mSv·h$^{-1}$·m$^2$) |
|---|---|
| 0 | 0.04 |
| 1 | 0.04 |
| 24 | 0.04 |
| 168 | 0.04 |
| 720 | 0.04 |
| 8760 | 0.03 |

It should be noted that in this case also the doses calculated represent a conservative approximation, as self-absorption has again been neglected.

*5.1.5. - Activated solid material storage*

The current scope of the accelerator does not involve, at least for the present, the production of active targets, so solid radioactive waste from the machine should only be from the machine components which will eventually be replaced during maintenance operations.

Generally, only objects with small volume and dimensions will be involved, so they will be storable in the same bunker where similar pieces from the linac presently operating are kept. The parts with larger dimensions can be left to decay in the accelerator room or in the access tunnel.

The procedure already followed for the currently operating machine will most likely be used to deal with the activated parts. This foresees a regulated control by the Health Physics Service of all the machine parts to be disassembled and/or removed from the plant. Any successive movement of objects resulting activated, including their eventual dumping after decay, will be supervised by the same Health Physics Service and noted down in a special register.

## 5.2. - Air in the accelerator room

The design study regarding air activation and the ventilation plant has been carried out using the model adopted for analogous estimates for the biomedical experimental cyclotron in Milan (Bi 84). Some modifications and integrations have, however, been introduced, as indicated in the following:

a) The ($\gamma$,n) reactions have been included to take account of the formation of 0-15 and N-13 which are the most important radionuclides produced by electron accelerators. The cross sections of the reactions are indicated in Table VIII. The characteristics of the X-ray sources (intensity, spectrum) are calculated using the EGS code (Fo 78) in the worst case of the beam being completely lost on a 1 cm-thick lead target.
b) The same neutron production hypothesized for the shielding calculation has been assumed, equal to $10^{12}$ $ns^{-1}$ $kW^{-1}$.
c) The waiting time before access is allowed to the LISA Hall has been fixed equal to the time necessary for the concentration of radionuclide mixture present to reach 1/10 of the MPC values.
d) The ventilation plant design has been studied hypothesizing that it operate ensuring three different states: during machine operation; in the period between machine shutoff and attainment of the concentration established at 1/10 of the MPC; after reaching the pre-established concentration.

In the extreme case of the machine operating for 3000 hours per year at full power (rounded off to 10 kW for simplicity), the model used gives the values in Table IX for the doses accumulated over a year at different distances from the plant. A rate of 0.1 changes per hour (c/h) has been assumed during machine operation, from 1 - 6 c/h during waiting time, and 6 c/h after the pre-established concentration has been reached. The contributions to the dose of the different radionuclides at 25 m and 50 m from the machine, respectively, are indicated in Table X. The largest contribution is from N-13 (between 73% and 77%), followed by O-15 (between 22% and 25%) and then A-41 (of the order of 1%), etc.

**TABLE VIII** - $^{14}N(\gamma,n)$ and $^{16}O(\gamma,n)$ reaction cross sections (from Ko 82).

| *Energy (MeV)* | *Cross sections (mb)* | |
|---|---|---|
| | $^{14}N(\gamma,n)$ | $^{16}O(<,n)$ |
| 10-11 | 0.018 | ------ |
| 11-12 | 0.158 | ------ |
| 12-13 | 0.438 | ------ |
| 13-14 | 0.526 | ------ |
| 14-15 | 0.333 | ------ |
| 15-16 | 0.404 | ------ |
| 16-17 | 0.175 | 0.159 |
| 17-18 | 0.596 | 1.034 |
| 18-19 | 1.491 | 0.604 |
| 19-20 | 1.842 | 1.352 |
| 20-21 | 1.702 | 1.082 |
| 21-22 | 1.754 | 2.863 |
| 22-23 | 2.825 | 7.364 |
| 23-24 | 2.747 | 6.392 |
| 24-25 | 1.649 | 6.998 |
| 25-26 | 1.081 | 5.853 |
| 26-27 | 0.807 | 4.453 |
| 27-28 | 0.607 | 3.817 |
| 28-29 | 0.421 | 3.022 |
| 29-30 | 0.267 | 2.465 |
| 30-31 | 0.175 | 1.588 |
| 31-32 | 0.070 | 1.082 |
| 32-33 | ------ | 0.375 |
| 33-34 | ------ | 0.188 |
| 34-35 | ------ | 0.188 |

**TABLE IX** - Annual dose equivalent due to air activation at various distances from the machine for different ventilation conditions between shutoff and reaching a radionuclide concentration equal to 1/10 of the MPC.

| *m* | *mSv/a (1c/h)* | *mSv/a (2c/h)* | *mSv/a (3c/h)* | *mSv/a (4c/h)* | *mSv/a (5c/h)* | *mSv/a (6c/h)* |
|---|---|---|---|---|---|---|
| 25 | 0.197 | 0.282 | 0.347 | 0.396 | 0.437 | 0.472 |
| 50 | 0.062 | 0.089 | 0.109 | 0.125 | 0.138 | 0.149 |
| 100 | 0.022 | 0.031 | 0.039 | 0.044 | 0.049 | 0.053 |
| 150 | 0.013 | 0.018 | 0.022 | 0.025 | 0.028 | 0.030 |
| 200 | $8.71\ 10^{-3}$ | 0.012 | 0.015 | 0.018 | 0.019 | 0.021 |
| 300 | $5.30\ 10^{-3}$ | $7.62\ 10^{-3}$ | $9.35\ 10^{-3}$ | 0.011 | 0.012 | 0.013 |
| 400 | $3.79\ 10^{-3}$ | $5.44\ 10^{-3}$ | $6.68\ 10^{-3}$ | $7.65\ 10^{-3}$ | $8.44\ 10^{-3}$ | $9.10\ 10^{-3}$ |

**TABLE X** - Contributions to the dose equivalent from the most important air activation products at 25 m and 50 m from the machine for different ventilation conditions between shutoff and reaching a concentration of the mixture in the accelerator room equal to 1/10 of the MPC.

| Nuclide | Dose equivalent (mSv/y) at 25 m and 50 from the machine | | | | | |
|---|---|---|---|---|---|---|
| | 1 c/h | 2 c/h | 3 c/h | 4 c/h | 5 c/h | 6 c/h |
| N-13 | 0.144 | 0.214 | 0.264 | 0.302 | 0.331 | 0.335 |
| | 0.046 | 0.068 | 0.084 | 0.096 | 0.106 | 0.113 |
| 0-15 | 0.050 | 0.065 | 0.079 | 0.091 | 0.103 | 0.114 |
| | 0.015 | 0.020 | 0.024 | 0.028 | 0.031 | 0.034 |
| A-41 | $2.53 \cdot 10^{-3}$ | $2.84 \cdot 10^{-3}$ | $2.97 \cdot 10^{-3}$ | $3.05 \cdot 10^{-3}$ | $3.10 \cdot 10^{-3}$ | $3.13 \cdot 10^{-3}$ |
| | $8.40 \cdot 10^{-4}$ | $9.40 \cdot 10^{-4}$ | $9.85 \cdot 10^{-4}$ | $1.01 \cdot 10^{-3}$ | $1.03 \cdot 10^{-3}$ | $1.04 \cdot 10^{-3}$ |

It should be noted, however, that the doses calculated above have been overestimated due to the conservative hypothesis introduced in the model and in the source description, and should result larger than the effective doses by at least a factor between 10 and 100, considering that the average operational power over the year is foreseen as being of the order of 1 kW and that only 10% can reasonably be supposed lost casually.

It should be recalled that in order to reduce the production of radioactive gases and any eventual toxic products such as ozone, etc., the beam path to the beam stops will pass inside metal guides.

The time from machine shutoff necessary for the radionuclide concentration in the accelerator to reach 1/10 of the MPC is given in Table XI as a function of the beam power and for the different ventilation conditions investigated. The same data are shown graphically in Fig. 11. In all cases, it has been assumed that the concentration reaches saturation values.

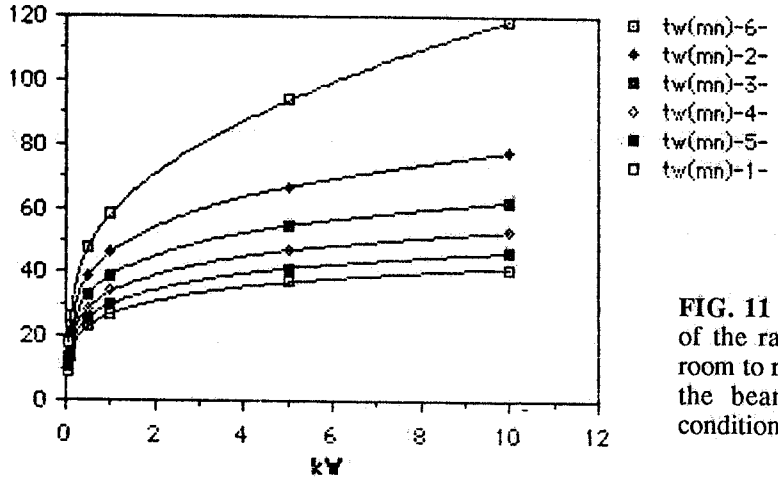


**FIG. 11** - Time required for the concentration of the radionuclide mixture in the accelerator room to reach 1/10 of the MPC as a function of the beam power for different ventilation conditions during the waiting time.

It is also to be observed that the above times are practically determined by the A-41, whose presence around electron accelerators is never very important. This is probably due to the overestimations introduced both in the calculation of the neutron source and in the ensuing deduction of the fluence of the thermal neutrons present.

**TABLE XI** - Times required for the concentration of the radionuclide mixture in the accelerator room to reach 1/10 of the MPC as a function of the beam power for different ventilation conditions during the waiting time.

| *kW* | $t_w$(*min*) *1c/r* | $t_w$(*min*) *2c/r* | $t_w$(*min*) *3c/r* | $t_w$(*min*) *4c/r* | $t_w$(*min*) *5c/r* | $t_w$(*min*) *6c/r* |
|---|---|---|---|---|---|---|
| 10 | 118.6 | 77.36 | 61.88 | 52.67 | 46.2 | 41.27 |
| 5 | 93.56 | 66.57 | 54.54 | 46.82 | 41.23 | 36.92 |
| 1 | 57.83 | 46.26 | 39.06 | 33.95 | 30.07 | 27.01 |
| 0.5 | 47.36 | 38.61 | 32.81 | 28.59 | 25.37 | 22.81 |
| 0.1 | 26.37 | 21.92 | 18.79 | 16.46 | 14.66 | 13.23 |
| 0.05 | 17.99 | 15.05 | 12.97 | 11.42 | 10.22 | 9.26 |

Considering the low doses values foreseen in the external areas in practically all the ventilation conditions examined, it has been decided to operate the ventilation plant in the following conditions to limit the waiting times before personnel can enter the accelerator room:

- during machine operation 0.1 changes/hour
- from shutoff 6 changes/hour

The waiting time required before entrance is allowed into the LISA Hall will be controlled by a timer which will prevent the entrances being opened for the time shown in Table XI, as a function of the machine power.

## 5.3. - Helium around the superconducting cavities

A further problem to be considered regarding activation, at least at the design stage, concerns the helium in the cryostat of the RF superconducting cavities. If the electromagnetic cascade develops in this element, tritium can be produced via the reaction:

$$\gamma + {}^4\mathrm{He} \longrightarrow p + T \qquad (12)$$

which has a threshold of 19.8 MeV.

If the target is thick enough to ensure the complete absorption of the cascade, one would have saturation activity of $1.87 \cdot 10^9 \mathrm{BqW}^{-1}$ (Sw 86). However, in the case of the LISA accelerator cavities, the helium occupies a much more limited thickness. The thickness available for the development of the cascade can be assumed of the order of 4 cm for each cell. As the complete development of the cascade requires 2.5 radiation lengths at least for an 80-100 MeV electron beam (e.g. Cr 62, La 63), and as the radiation length of helium is about 755 cm, the fraction of the cascade which develops in 4 cm is of the order of $2.10^{-3}$.The saturation activity, which would only be reached after some tens of years, would therefore be of the order of $3.7 \cdot 10^6$ Bq/W. As there are 16 cavities, the total would be $6 \cdot 10^7$ Bq/W.

With regard to the possible losses along the straight section of the machine, where the SC cavities are installed, it should be noted that the losses are kept at extremely low levels so that 2-3 W/cm$^2$ per cavity can cause quenching. Analogous to the assumptions made for the CEBAF project (CEBAF 86), the loss of only one watt for each SC cavity will be hypothesized in the following. The total saturation activity will therefore be $6 \cdot 10^7$ Bq.

The transformation of tritium in helium does not give rise to any problems of external irradiation. The only risk worth considering is an eventual incidental loss from one of the multicells. The quantity of tritium that would be expelled in the air is therefore given by:

$$A_{exp} = A_{tot} \times \text{He vol. in a multicell/total He vol.} \qquad (13)$$

The volume of helium per multicell is about 100 l, and the total volume about 500 l, so $A_{exp}$ would be $1.2 \cdot 10^7$ Bq. The concentration in the accelerator room would be $4.3 \cdot 10^3$ Bq m$^{-3}$ . It is useful to compare this concentration with the DAC recommended by the ICRP (ICRP 78) for 2000 working hours/year, which are $8 \cdot 10^5$ Bq m$^{-3}$ for inhalation of tritium water and $2 \cdot 10^{10}$ Bq m$^{-3}$ for submersion in elemental tritium-contaminated air .

## 5.4. - Cooling circuit water

The cooling circuit mainly serves the injector and the ondulator magnet. It is a closed circuit containing demineralized water with a capacity of 14 m$^3$/h. The water heat exchanger is in the generator room.

The radionuclides which can form in the water following induced photon reactions are listed in Table XII, together with some parameters important for the protection aspects.

**TABLE XII** - Photoactivation products of O-16 in water (from Sw 79).

| Nuclide | $T_{\frac{1}{2}}$ | $MPC_w$ [a] (Bq·cm$^{-3}$) | $\Gamma$ [b] Specific gamma-ray constant ((fC·kg$^{-1}$·h$^{-1}$)(Bq·m$^{-2}$)$^{-1}$) | Reaction type | Threshold (MeV) | Cross-section [c] $\sigma_{-2}$ ($\mu$b·MeV$^{-1}$) | $A_s$ [c,d] Saturation activity (GBq·kW$^{-1}$) |
|---|---|---|---|---|---|---|---|
| O-15 | 123 s | – | 4.11 ($\beta^+$) | ($\gamma$,n) | 15.67 | 75 | 330 |
| O-14 | 70.91 s | – | 11.16 ($\beta^+$) | ($\gamma$,2n) | 28.89 | (1) | (3.7) |
| N-13 | 9.96 min | – | 4.11 ($\beta^+$) | ($\gamma$,2np) | 25.02 | 0.9 | 3.7 |
| C-11 | 20.34 min | – | 4.11 ($\beta^+$) | ($\gamma$,3n2p) | 25.88 | 3 | 15. |
| C-10 | 19.48 s | – | 7.04 ($\beta^+$) | ($\gamma$,4n2p) | 38.10 | (1) | (3.7) |
| Be-7 | 53.6 d | 740 | 0.20 – | ($\gamma$,5n4p) | 31.86 | 0.3 | 1.5 |
| H-3 | 12.262 a | 1110 | – ($\beta^-$) | ($\gamma$,H-3) | 25.02 | 1.5 | 7.4 |

[a] ICRP recommendation for the general public, 168-hour week occupancy. See text for discussion.
[b] See Footnote 14 (Section 2.6).
[c] Values in parentheses are rough estimates.
[d] Saturation activity in water per unit electron beam power. Assume 100% direct absorption of electron beam power in water. Activity in water will be less in most situations where the beam absorber is water-cooled metal. Values shown are obtained directly from Approximation A and apply at high energies. For $E_0 \gtrsim 50$ MeV, the value for O-15 may be reduced by a factor of two, and others by an even larger factor.

As the ducts for the tubes have not been completely defined at the present design phase, no evaluation has yet been made. Furthermore, this is considered a secondary problem compared to those so far examined, especially in view of the fact that the tube ducts will not concern the external areas.

## 6. - INTERLOCKS AND WARNING DEVICES

The safety system will follow the general criteria normally used for particle accelerators.

It will consist of highly reliable and long-life components. When the latter are installed in areas where high radiation levels are expected, their resistance against radiation effects will also be taken into account.

As far as possible the components will be of the fail-safe type.

The apparatus for the control logic of the safety system will be installed in special locked cabinets.

The various circuits and mechanisms necessary to block the accelerator will operate independently of one another. When possible, beam shutoff will be effected using at least two methods.

The efficiency of the various components of the safety system will be checked periodically (every six months) and in the case of any maintenance work under the supervision of the radiation safety specialist.

The details of the safety system are as follows:

1. Luminous display boards will be installed near each entrance to the accelerator room, inside the room, and in the generator room and control room, indicating the operational status of the machine and reading as follows: MACHINE off, Controls on, High Voltage, and Accelerated Electrons.
2. Red lights in the generator and accelerator rooms will flash to indicate that one or more modulators are ready for switching on the high voltage and that the entrance doors to the accelerator room are closed. The lights will remain lit when one or more modulators are operating at high voltage.
3. Each modulator will have a green light to indicate that the controls are on, and a red one to indicate high voltage.
4. The accelerator room will have a main entrance through a sliding door and a service entrance, both communicating with the outside via labyrinths and stairways.
5. If either of the two doors along the labyrinths are opened (one opening towards the outside and one onto accelerator room), the accelerator will not operate and power will not be supplied to the superconducting cavities. This will be assured by two independently-wired double microswitches installed on each door. The entrance doors will have fixed key locks. If any of the

keys is taken from its place in the control room, accelerator operation and power to the superconducting cavities is prevented.

6. The opening of the doors referred to in point 5, will be controlled by a timer synchronized according to the waiting times reported in Table XI. A push-button enclosed in a glass-panelled cabinet will be installed beside each of the two doors to the accelerator room. In an emergency situation, the panel is to be broken and pushing the button allows the door to be opened immediately.
7. Both entrances will be controlled by an electromechanic system operated by magnetic cards at exit and entrance.
8. After maintenance operations involving removal of the electromechanical system referred to in point 7, an inspection will be carried out by the operators , and machine operation will be resumed by resetting the push-buttons distributed opportunely inside the accelerator room.
9. An audible warning will sound for about 30 seconds just before the last door in the accelerator room is shut.
10. Emergency push-buttons to shut off the accelerator controls power supply and, therefore, the beam, the high voltage and the power supply to the superconducting cavities, will be located in the accelerator and machine rooms. The same buttons used for the shutoff must be pushed to resume machine operation.
11. The machine and safety system operational status will be displayed on a synoptic panel in the control room.

## 7. - RADIATION MONITORING SYSTEM

The radiation control of the machine will be carried out by means of active and passive detectors.

A pair of detectors for gamma rays and for neutrons will be located in all the areas normally open to access by personnel. As very low doses are expected in these areas (see sect. 4), the detectors will have a mainly psychological function.

A device will be installed in the plant for controlling the activity of the air expelled to the outside environment.

A control network will be located in all the rooms and in the external surrounding areas consisting of passive detectors, thermoluminescence dosimeters for the photon radiation, and combination dosimeters (CR 39 and albedo detectors) for the neutron radiation.

The above controls may be subject to change consequent to the project development and to technological research.

# 8. - EVALUATION OF RADIOLOGICAL RISK TO PERSONNEL AND POPULATION DUE TO MACHINE OPERATION

## 8.1. - Normal working conditions

It appears evident from the preceding Sections 4 and 5 that the doses in the various work areas, apart from the LISA Hall, and in the areas outside the laboratories will be extremely limited and in any case lower than the values detectable with the instruments used for personnel monitoring.

The most notable doses received by personnel will be relative to maintenance operations carried out in the presence of activated materials, as is the case for all accelerator machines. It is helpful in this regard to utilize the experience gained from the 40-kW linac currently operating at the LNF, where only a limited number of personnel need be involved in maintenance, receiving a dose equivalent of the order of a few mSv/year. This could equally be applied to the new machine, imposing the same control over the maintenance work (carried out under the direct supervision of a radiation safety specialist who will establish the waiting and operational times, protection measures and personnel monitoring).

## 8.2. - Accident conditions

The only type of radiation accident that can be hypothesized would be the accidental irradiation of someone inside the LISA Hall during accelerator operation. This could be extremely serious, but is highly improbable because of the redundancy in the safety system (see Sect. 6). As the electron beam travels completely inside vacuum guides, if such an event should ever occur, the person involved would not be exposed to a primary beam but to secondary radiation (X rays and neutrons) produced by the beam on the machine structures.

An a priori evaluation of the absorbed dose is practically impossible, partly because of the erratic nature of the radiation field due to the beam loss distribution, and partly because it would be impossible to establish the duration and mode of exposure (due to the casual presence of shields, movement of people,etc.).

An extreme value of the dose levels potentially present can usually be obtained referring to losses onto a hypothetical target having optimal thickness for the production of secondary radiation. In this case, the dose levels that could result around the target are:

| | | |
|---|---|---|
| - X rays in the direction at $0^o$ | ~385 | Gy $min^{-1}$ $m^2$ $kW^{-1}$ |
| - X rays in the direction at $90^o$ | ~0.4 | Gy $min^{-1}$ $m^2$ $kW^{-1}$ |
| - fast neutrons in all the directions | ~0.02 | Gy $min^{-1}$ $m^2$ $kW^{-1}$ |

On the other hand, under the hypothesis of a thin target, e.g., of the order of 0.01 $X_0$ , only 1% of the beam would be lost, with a neutron production equal to about $10^{-4}$ times that occurring on a thick target. The source terms would then be:

| | | |
|---|---|---|
| - X rays in the direction at 0° | ~ 3.85 | Gy $min^{-1}$ $m^2$ $kW^{-1}$ |
| - X rays in the direction at 90° | ~ 4 | mGy $min^{-1}$ $m^2$ $kW^{-1}$ |
| - fast neutrons in all the directions | ~ 2 | μGy $min^{-1}$ $m^2$ $kW^{-1}$ |

## 9. - AREA CLASSIFICATION

Subject to confirmation after experimental measurements, the areas will be classified as follows:

| | |
|---|---|
| - LISA Hall (including entrance labyrinths) | Exclusion area when accelerator operating.<br>Controlled area when accelerator shut off. |
| - Generator room | Controlled area |
| - Control room | Supervised area |
| - Technical workshops | Supervised area |

## REFERENCES


Bi 84 C. Birattari, M. Bonardi, A. Ferrari e M. Silari, Il progetto ciclotrone per usi biomedici di Milano: valutazione sull'attivazione indotta nell'aria, INFN/TC-84/29 (1984).

CEBAF 86 Continuous Electron Beam Accelerator Facility (CEBAF), Workshop on radiation safety (1986).

CERN 84 A. Fassò, K. Goebel, M. Höfert, G. Rau, H. Schönbacher, G.R. Stevenson, A.H. Sullivan, W.P. Swanson and J.W.N. Tuyn, Radiation problems in the design of the large electron-positron collider (LEP) - CERN 84-02 (1984).

Cr 62 J.W. Cronin, E. Engels, M. Pyka and R. Roth, Electron showers in a lead plate spark chambers, The Review of Scientific Instruments, 33, 946 (1962).

Fa 87 A. Fassò, The CERN version of MORSE and its application to strong-attenuation shielding problems, Proceedings of Theory and practices in radiation protection and shielding, Knoxwille (1987).

Fo 78 R.L. Ford and W.R. Nelson, The EGS code system: computer programs for the Monte Carlo simulation of electromagnetic cascade shower (version 3), SLAC 210, UC-32 (1978).

IAEA 79 International Atomic Energy Agency, Radiological safety aspects of the operation of electron linear accelerators, Technical reports series N. 188 (1979).

ICRP 78 International Commission on Radiological Protection, Limits for intakes of radionuclides by workers, ICRP Publication 30, Supplement to Part 1, Pergamon Press, Oxford (1978).

ICRP 85 International Commission on Radiological Protection, Statement from the 1985 Paris meeting of the International Commission on Radiological Protection, ICRP Publication 45, Pergamon Press, Oxford (1985).

ICRP 87 International Commission on Radiological Protection, Data for use in protection against external radiation, ICRP Publication 51, Annals of the ICRP, 17, No 2/3 (1987).

ICRU 86 International Commission on Radiation Units and Measurements, The quality factor in radiation protection, ICRU Report 40 (1986).

Ko 82 T. Kosako and T. Nakamura, Air activation by an electron accelerator, Health Physics 43, 3 (1982).

La 63 H. Lengeler, W. Tejessy und M. Deutschmann, Messungen von Elektroneuschauern in Blei und Kupfer mit Hilfe einer Blasenkammer, Zeitschrift für Physick, 175, 283 (1963).

St 87 G.R. Stevenson, Neutron attenuation in labyrinths, ducts and penetrations at high energy proton accelerators, Proceedings of Theory and practices in radiation protection and shielding, Knoxville (1987).

Sw 85 W.P. Swanson, P.M. De Luca, R.A. Otte and S.W. Schilthelm, Aladdin upgrade design study: shielding (1985).

Sw 86 W.P. Swanson, Photoproduction of tritium in helium cryostats at electron accelerators, in CEBAF 86.

Te 82 K.Tesch, The attenuation of the neutron dose equivalent in a labyrinth through an accelerator shield, Particle Accelerators, Vol. 12, pag. 169 (1982).

Te 87 K. Tesch, Attenuation of the photon dose in labyrinths and ducts at accelerators, Rad. Prot. Dos., Vol. 20, No 3, 131, 1987.